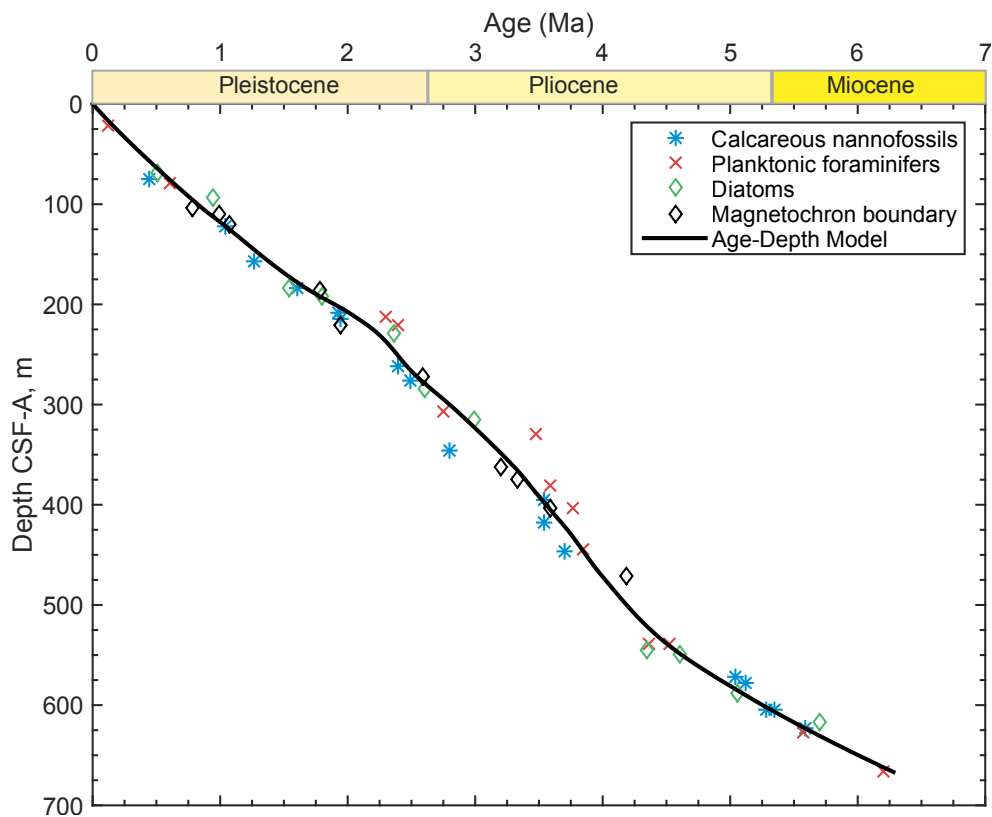


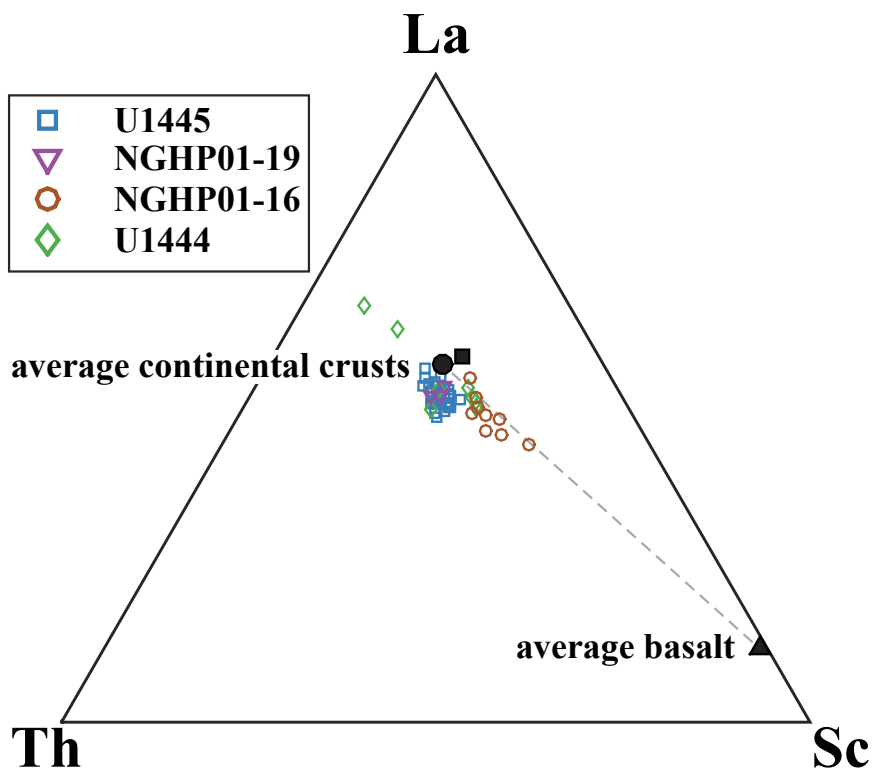
## Supplemental Material

435 Figure S1. Age-depth model for Site U1445. To determine the ages of our samples, we fit the biostratigraphic and magentostratigraphic age constraints (Clemens et al., 2016) with an age-depth model using CLAM software in R (Blaauw, 2010). We ran iterations of the model with different types of fit and levels of smoothing, and identified a locally weighted spline with 0.4 smoothing to best represent the trends observed in the age constraints. The differences between the age models iterations are not significant and would not change the interpretations of this study.



440 Figure S2. La-Th-Sc diagram of 30 sediment samples from the Bay of Bengal. Samples from IODP Site U1445 (blue squares) are plotted as well IODP Site U1444 (green diamonds), NGHP Site 19 (purple triangles), and NGHP Site 16 (brown circles) in the Bay of Bengal. Average upper continental crust (black square, Rudnick and Gao, 2014), post-Archean average Australian Shale (black dot, Taylor and McLennan, 1985), and average mid-ocean ridge basalt (Gale et al., 2013) compositions are plotted for reference.

445



450 **Figure S3. Carbonate and bulk organic analyses at Site U1445. Analysis of 57 samples at IODP Site U1445 for (a) bulk calcium carbonate content (weight %) calculated as (total inorganic carbon x (8.33313 CaCO<sub>3</sub> wt/C wt)), (b) total organic carbon concentration (weight %), (c) total acidified nitrogen content (weight %), (d) Ratio of total organic carbon to total nitrogen (TOC/TN, wt.%/wt.%) and (e) carbon isotopes of the total organic carbon (per mil). Black dots represent visually darker layers relative to a lighter layer (white dot) at a similar depth. TOC/TN shows a distinct increase in the mid-Pliocene, but remains within the range of TOC/TN expected for marine organic material.**

455

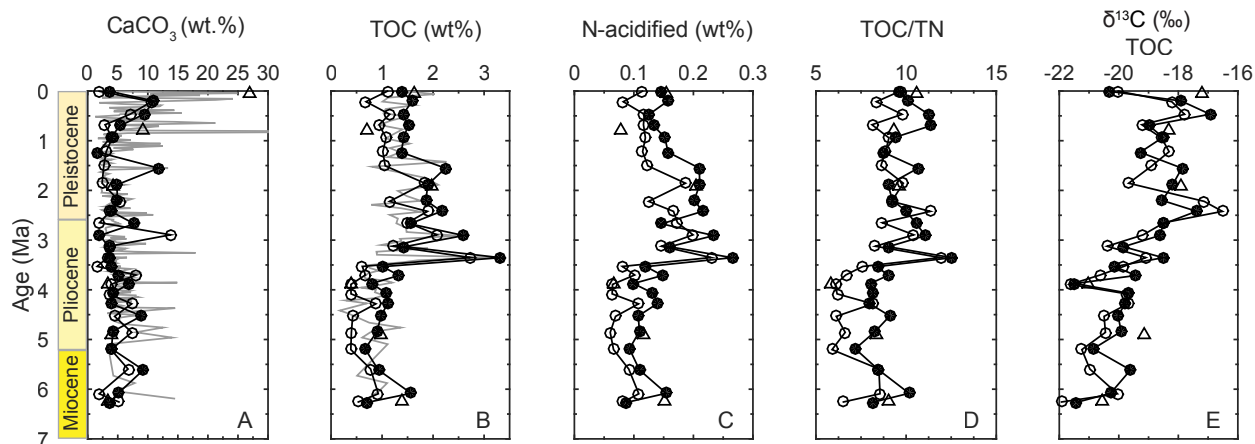
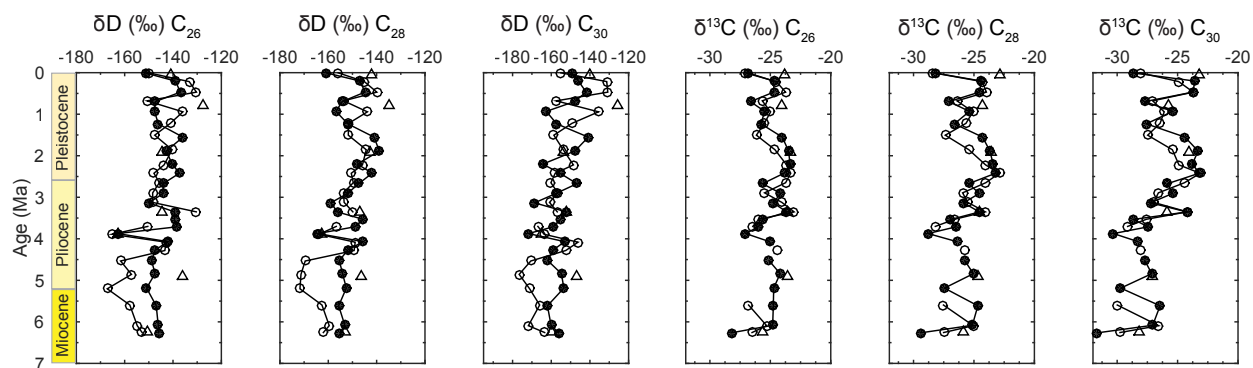


Figure S4. Long-chain fatty acids from leaf waxes extracted from Site U1445. Plotted from left to right are hydrogen isotopes and then carbon isotopes of leaf wax fatty acids from chainlengths C<sub>26</sub>, C<sub>28</sub>, and C<sub>30</sub>.

460

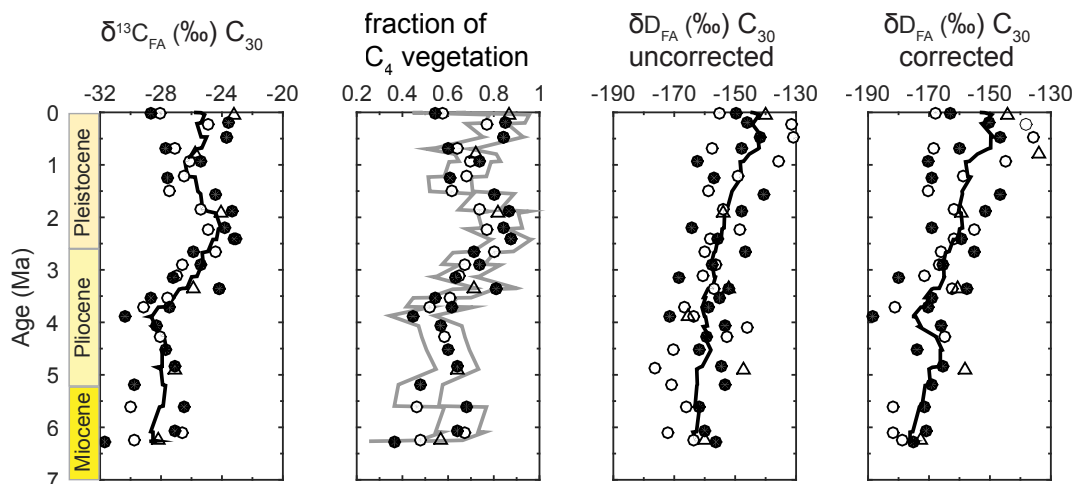


465 Figure S5. Correcting  $\delta D$  for differences in fractionation due to plant physiology. (a) Raw, uncorrected  $\delta^{13}C_{FA}$  plotted for comparison. (b) Calculated fraction of  $C_4$  vegetation with grey lines indicating the maximum and minimum boundaries. (c) Uncorrected  $\delta D$  data, plotted here for comparison. (d) The  $\delta D$  data corrected for differences between  $C_3$  and  $C_4$  plant physiologies.

470 We used the  $\delta^{13}C_{FA}$  to calculate the relative percentages of  $C_3$  and  $C_4$  vegetation and then correct the  $\delta D$  for differences in plant physiology (Smith and Freeman, 2006; Chikaraishi and Naraoka, 2007). For consistency with other studies in proximity to our marine sediment site, we used the end-member values of Ponton et al. (2012). They used values reported in Chikaraishi et al. (2004) extracted from 52 measurements of  $\delta^{13}C$  for n-alkanoic acids isolated from different plant species of  $C_3$  plants between  $C_{26}$  and  $C_{32}$  averaging  $-37.7 \pm 1.8 \text{ ‰}$  and 16 measurements of the same compounds in  $C_4$  plants with an average of  $-21.1 \pm 1.4 \text{ ‰}$ . We use these same end-member values [ $-37.7 \text{ ‰} = 0\% C_4$  plants;  $-21.1 \text{ ‰} = 100\% C_4$ ], to calculate our  $\delta^{13}C$  plant wax values as a percentage of  $C_4$  plants. The maximum and minimum fractions of  $C_4$  vegetation (gray lines) were calculated with the standard deviation of  $\delta^{13}C$  within the  $C_3$  and  $C_4$  groups (Ponton et al., 2012).

475 We estimate the offset in  $\delta D$  between  $C_3$  and  $C_4$  plants to be  $\sim 25\text{‰}$  (Smith and Freeman, 2006; Ghosh et al., 2017) where  $C_3$  is on average 25 ‰ lighter than  $C_4$  vegetation. Using the fraction of  $C_4$  relative to  $C_3$  estimated from the  $\delta^{13}C_{FA}$ , we correct the  $\delta D$  of each sample for the differences in plant physiology.

480 The corrected data shows the same overall trend as the uncorrected data, except the values are shifted to be more negative and the change in  $\delta D$  between  $\sim 3.5$  and  $\sim 1.5$  Ma is steeper. Thus, the correction emphasizes the drying trend that we interpret in the data. Since we are interpreting  $\delta D$  as a qualitative proxy for aridity or the relative amount of precipitation, the slope of the  $\delta D$  change has no impact on our interpretations of the data. The corrected  $\delta D$  data is discussed in the main text of the manuscript.



485

Table S1. Concentrations of major, trace, and rare earth elements. Inorganic analyses of major, trace, and rare earth element concentrations for 30 bulk sediment samples at Site U1445 and additional samples from other sites in the Bay of Bengal for reference. For methods see Appendix A or details in Dunlea et al. (2015).

490 Table S2. Carbonate and bulk organic analyses data at Site U1445. Analysis of 57 samples at Site U1445 for bulk calcium carbonate, total organic carbon, total carbon, total acidified nitrogen, carbon isotopes of the total organic carbon, and the designation of visually lighter versus darker samples at similar depths.

495 Table S3. Carbon and hydrogen isotope analysis of leaf wax fatty acids at Site U1445. Hydrogen isotopes and carbon isotope analyses of leaf wax fatty acids extracted from 57 samples at Site U1445. Measurements from fatty acid chainlengths C<sub>26</sub>, C<sub>28</sub>, and C<sub>30</sub> are reported with their standard deviation. The correction for C<sub>3</sub>-C<sub>4</sub> physiological differences in the hydrogen isotopes of C<sub>30</sub> fatty acids is reported, estimating C<sub>3</sub> vegetation as having a δ<sup>13</sup>C of -35.4 ‰ and C<sub>4</sub> vegetation as -21.4‰ (Fig. S5).







Supplemental Table S2

Exp	Site	Hole	Core	Type	Sect	W	Top	Bot	Depth	Age	CaCO <sub>3</sub>	Total Organic C	Total Carbon	Total N, acidified	δ <sup>13</sup> C, TOC	Color
									mbsf, CFA	Ma	wt. %	wt. %	wt. %	wt. %	per mill	relative to pair
353	U1445	A	1	H	1	W	41	43	0.41	0.00	1.93	1.11	1.34	0.11	-20.02	Light
353	U1445	A	1	H	1	W	93	95	0.93	0.01	1.39	1.39	1.82	0.14	-20.30	Dark
353	U1445	A	1	H	5	W	23	25	6.23	0.04	2.61	1.64	4.86	0.16	-17.23	No Pair
353	U1445	A	4	H	1	W	100	102	28.9	0.20	11.04	1.59	2.91	0.16	-17.80	Dark
353	U1445	A	4	H	2	W	120	122	26.6	0.21	10.62	0.69	1.96	0.08	-18.22	Light
353	U1445	A	7	H	4	W	92	94	59.43	0.47	9.35	1.41	2.34	0.13	-16.93	Dark
353	U1445	A	7	H	4	W	112	114	59.63	0.47	7.02	1.15	1.99	0.12	-17.79	Light
353	U1445	A	10	H	1	W	95	97	83.85	0.68	2.88	0.94	1.29	0.12	-19.23	Light
353	U1445	A	10	H	3	W	41	43	85.88	0.70	5.42	1.51	2.16	0.13	-18.98	Dark
353	U1445	A	11	H	4	W	61	63	96.82	0.80	9.21	0.72	1.83	0.08	-18.33	No Pair
353	U1445	A	12	H	8	W	37	39	111.22	0.93	3.83	1.43	1.89	0.15	-18.52	Dark
353	U1445	A	13	H	1	W	88	90	112.28	0.94	4.09	1.08	1.57	0.12	-18.36	Light
353	U1445	A	16	H	1	W	70	72	140.6	1.22	3.07	1.02	1.38	0.11	-18.31	Light
353	U1445	A	16	H	2	W	65	67	141.81	1.23	1.72	1.38	1.58	0.16	-19.28	Dark
353	U1445	A	19	H	1	W	70	72	169.1	1.51	2.68	1.06	1.38	0.12	-18.89	Light
353	U1445	A	19	H	4	W	78	80	173.35	1.55	11.80	2.24	3.66	0.21	-17.88	Dark
353	U1445	A	22	H	1	W	30	32	197.2	1.86	2.39	1.84	2.12	0.19	-19.67	Light
353	U1445	A	22	H	2	W	93	95	199.33	1.89	4.86	1.90	2.48	0.21	-18.19	Dark
353	U1445	A	22	H	4	W	88	90	201.6	1.92	4.32	1.96	2.48	0.20	-17.90	No Pair
353	U1445	A	25	X	1	W	41	43	225.51	2.20	4.95	1.86	2.45	0.20	-18.54	Dark
353	U1445	A	28	X	3	W	12	14	227.5	2.22	5.33	1.15	1.79	0.12	-17.13	Light
353	U1445	A	28	X	1	W	104	106	255.24	2.42	3.83	2.16	2.62	0.22	-17.39	Dark
353	U1445	A	28	X	1	W	138	140	255.58	2.42	3.74	1.89	2.34	0.17	-16.52	Light
353	U1445	A	31	X	1	W	59	61	283.89	2.65	1.97	1.50	1.74	0.17	-18.48	Light
353	U1445	A	31	X	3	W	40	42	286.41	2.67	7.76	1.55	2.48	0.15	-18.49	Dark
353	U1445	A	34	X	1	W	19	21	310.89	2.89	13.81	2.08	3.73	0.20	-18.18	Light
353	U1445	A	34	X	2	W	53	55	312.64	2.91	1.98	2.60	2.84	0.23	-18.63	Dark
353	U1445	A	37	X	4	W	82	84	338.75	3.12	3.58	1.21	1.64	0.15	-20.39	Light
353	U1445	A	37	X	5	W	53	55	339.97	3.13	3.50	1.44	1.86	0.16	-19.84	Dark
353	U1445	A	41	X	1	W	117	119	368.97	3.35	3.29	2.73	3.13	0.23	-19.09	Light
353	U1445	A	41	X	2	W	11	13	368.93	3.35	3.63	3.32	3.76	0.26	-18.51	Dark
353	U1445	A	44	X	4	W	61	63	396.06	3.53	1.57	0.61	0.80	0.08	-19.83	Light
353	U1445	A	44	X	4	W	136	138	396.81	3.53	3.88	1.01	1.48	0.12	-20.15	Dark
353	U1445	A	47	X	5	W	84	86	422.01	3.70	8.07	0.67	1.64	0.10	-20.63	Light
353	U1445	A	48	X	1	W	8	10	423.48	3.71	5.04	1.33	1.93	0.15	-19.42	Dark
353	U1445	A	51	X	4	W	74	76	451.55	3.87	6.88	0.80	1.62	0.10	-21.47	Dark
353	U1445	A	51	X	6	W	135	137	454.63	3.89	3.85	0.39	0.85	0.06	-21.64	Light
353	U1445	A	51	X	8	W	6	8	455.77	3.90	3.26	0.39	0.78	0.07	-21.04	No Pair
353	U1445	A	55	X	4	W	15	17	482.78	4.07	4.24	1.08	1.59	0.13	-19.68	Dark
353	U1445	A	55	X	5	W	69	71	484.82	4.08	3.52	0.39	0.81	0.06	-19.74	Light
353	U1445	A	59	X	2	W	57	59	512.37	4.27	3.80	1.11	1.57	0.14	-19.79	Dark
353	U1445	A	59	X	3	W	12	14	513.43	4.28	7.32	0.88	1.76	0.11	-19.70	Light
353	U1445	A	62	X	4	W	133	135	541.21	4.53	8.94	0.98	2.05	0.11	-20.02	Dark
353	U1445	A	62	X	5	W	68	70	542.06	4.53	4.47	0.42	0.96	0.07	-20.49	Light
353	U1445	A	66	X	1	W	106	108	568.46	4.84	4.17	0.90	1.40	0.11	-19.92	Dark
353	U1445	A	66	X	2	W	90	92	569.81	4.86	7.32	0.40	1.28	0.06	-20.45	Light
353	U1445	A	69	X	4	W	80	82	572.53	4.89	4.03	0.98	1.47	0.12	-20.13	No Pair
353	U1445	A	69	X	4	W	25	27	595.05	5.19	3.97	0.66	1.14	0.09	-19.86	Dark
353	U1445	A	71	X	1	W	148	150	596.28	5.20	3.88	0.39	0.85	0.07	-21.24	Light
353	U1445	A	71	X	7	W	63	65	623.54	5.59	6.71	0.78	1.58	0.09	-20.97	Light
353	U1445	A	72	X	1	W	90	92	624.8	5.61	9.26	0.93	2.04	0.11	-19.61	Dark
353	U1445	A	75	X	4	W	62	64	654.8	6.08	5.08	1.57	2.18	0.15	-20.28	Dark
353	U1445	A	75	X	4	W	121	123	655.39	6.09	1.91	0.93	1.16	0.11	-20.05	Light
353	U1445	A	76	X	4	W	79	81	664.72	6.25	3.35	1.38	1.78	0.15	-20.57	No Pair
353	U1445	A	76	X	5	W	28	29	665.33	6.26	5.19	1.16	1.16	0.08	-21.92	Light
353	U1445	A	76	X	5	W	73	75	665.78	6.26	3.66	0.72	1.16	0.09	-21.42	Dark



## References for Supplemental Material

- 505 Blaauw, M.: Methods and code for 'classical' age-modeling of radiocarbon sequences, *Quat. Geochron.*, 5, 512-518, doi:10.1016/j.quageo.2010.01.002, 2010.
- Chikaraishi, Y. and Naraoka, H.:  $\delta^{13}\text{C}$  and  $\delta\text{D}$  relationships among three n-alkyl compound classes (n-alkanoic acid, n-alkane and n-alkanol) of terrestrial higher plants, *Org. Geochem.*, 38(2), 198–215, doi:10.1016/j.orggeochem.2006.10.003, 2007.
- 510 Chikaraishi, Y., Naraoka, H. and Poulson, S. R.: Hydrogen and carbon isotopic fractionations of lipid biosynthesis among terrestrial ( $\text{C}_3$ ,  $\text{C}_4$  and CAM) and aquatic plants, *Phytochemistry*, 65(10), 1369–1381, doi:10.1016/j.phytochem.2004.03.036, 2004.
- Clemens, S. C., Kuhnt, W., LeVay, L. J., Anand, P., Ando, T., Bartol, M., Bolton, C. T., Ding, X., Gariboldi, K., Giosan, L., Hathorne, E. C., Huang, Y., Jaiswal, P., Kim, S., Kirkpatrick, J. B., Littler, K., Marino, G., Martinez, P., Naik, D.,
- 515 Peketi, A., Phillips, S. C., Robinson, M. M., Romero, O. E., Sagar, N., Taladay, K. B., Taylor, S. N., Thirumalai, K., Uramoto, G., Usui, Y., Wang, J., Yamamoto, M. and Zhou, L.: Indian Monsoon Rainfall, *Proc. of IODP*, 353, doi:10.14379/iodp.proc.353.101.2016, 2016.
- Dunlea, A. G., Murray, R. W., Sauvage, J., Spivack, A. J., Harris, R. N. and D'Hondt, S.: Dust, volcanic ash, and the evolution of the South Pacific Gyre through the Cenozoic, *Paleocean.*, 30, 1078–1099, doi:10.1002/2015PA002829,
- 520 2015.
- Gale, A., Dalton, C. A., Langmuir, C. H., Su, Y. and Schilling, J.-G.: The mean composition of ocean ridge basalts, *Geochem. Geophys. Geosy.*, 14(3), 489–518, doi:10.1029/2012GC004334, 2013.
- Ghosh, S., Sanyal, P. and Kumar, R.: Evolution of  $\text{C}_4$  plants and controlling factors: Insight from n-alkane isotopic values of NW Indian Siwalik paleosols, *Org. Geochem.*, 110, 110–121, doi:10.1016/j.orggeochem.2017.04.009, 2017.
- 525 Ponton, C., Giosan, L., Eglinton, T. I., Fuller, D. Q., Johnson, J. E., Kumar, P. and Collett, T. S.: Holocene aridification of India, *Geophys. Res. Lett.*, 39(3), L03704, doi:10.1029/2011GL050722, 2012.
- Rudnick, R. L. and Gao, S.: Composition of the Continental Crust, in *Treatise on Geochemistry*, edited by H. Holland and K. Turekian, pp. 1–51, Elsevier Ltd., 2014.
- Smith, F. A. and Freeman, K. H.: Influence of physiology and climate on  $\delta\text{D}$  of leaf wax n-alkanes from  $\text{C}_3$  and  $\text{C}_4$  grasses, *Geochim. Cosmochim. Acta*, 70(5), 1172–1187, doi:10.1016/j.gca.2005.11.006, 2006.
- 530 Taylor, S. R. and McLennan, S. M.: *The Continental Crust: Its Composition and Evolution*, Blackwell Scientific Publications Inc., Oxford. 1985.